EARTH ANALOGUE TESTING AND ANALYSIS OF MARTIAN DURICRUST PROPERTIES

William Lewinger [(1)], Francisco Comin [(1)], Marcus Matthews [(1)], Chakravarthini Saaj [(1)]

[(1)] University of Surrey, Guildford, Surrey, GU2 7XH, United Kingdom, Email: w.lewinger@dundee.ac.uk

ABSTRACT

Previous and current Mars rover missions have noted a nearly ubiquitous presence of duricrusts on the planet surface. Duricrusts are thin, brittle layers of cemented regolith that cover the underlying terrain. In some cases, the duricrust hides a safe, or relatively safe, soil. However, as was observed by both MER rovers, Spirit and Opportunity, such crusts can also hide loose, untrafficable terrain, leading to Spirit becoming permanently incapacitated in 2009. Whilst several reports of the Martian surface have indicated the presence of duricrusts, none have been able to provide details on the physical properties of the material. This paper presents the findings of testing terrestrially-created duricrusts with simulated Martian soil properties. Combinations of elements that have been observed in the Martian soil were used as the basis for forming the laboratory-created duricrusts. Variations on duricrust thickness, water content, and the iron oxide compound were investigated. As was observed throughout the testing process, duricrusts behave in a rather brittle fashion and are easily destroyed by low surface pressures. This indicates that duricrusts present a definite hazard to traversing the Martian landscape when utilising only visual terrain classification, as the surface appearance is not necessarily representative of what may lie beneath.

1. INTRODUCTION

Mars is an intriguing destination within the solar system as a possible host for past life or the presence of life-essential building blocks. This makes our close neighbour an enticing candidate for remote exploration. For the past 50 years, several missions have been sent to Mars (Fig. 1) to collect data in the hope of further our understanding of the universe, each with varying success. The NASA Mariner missions during the mid-1960's brought the first close-up images of the Martian surface from orbit, along with atmospheric and temperature data. Additional orbiter data were provided by the U.S.S.R. "Mars" missions in the early 1970's, along with a successful landing on the surface in 1971. The Mars 3 lander was equipped with sensor equipment and an autonomous rover (PROP-M), which was a very promising mission [1]. Unfortunately, the lander was only operational for about 14.5s before ceasing transmissions [2]. In the mid-to-late 1970's the NASA Viking missions successfully landed on the planet

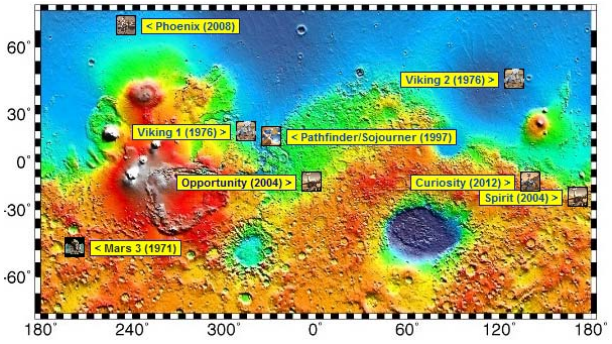

Figure 1. Martian elevation map showing the successful lander and rover mission touchdown sites [2].

surface and reported on chemical composition of the soil [4]. It also provided the first hints at possible former life on Mars. More recently, several rover, lander, and orbiter missions have successfully reached Mars. The modern rovers and landers: Pathfinder, Spirit, Opportunity, Phoenix, and most-recently, Curiosity have so far travelled more than 70km [5][6], combined, analysing the Martian atmosphere, soil, and rocks to gather scientific data, specifically concerning the possible existence of past life on the planet. Each of these missions has directly or indirectly experienced sulphate salt-based duricrusts [3] across the surface of Mars during their missions (Fig. 1).

Due to their longer-than-expected operational performance, the NASA Mars Exploration Rovers (MER) Spirit and Opportunity have been incredibly successful. Initially intended for 90-day missions, both of the rovers have been on Mars for just over 10 years, with Opportunity still operational and gathering data. In 2005, however, Opportunity became lodged in the soft soil underlying a thin surface duricrust at "Purgatory Dune" [5]. As seen in Fig. 2, there is a thin duricrust layer on the surface that obscures the underlying regolith, which for this area is of a different composition than the surface material. This obscuring effect is a danger when navigating by vision-based means for terrain classification, since it is unknown what type of terrain is actually present beneath the surface. In May 2009, Spirit suffered a similar "embedding event".

For each of these cases, the initial embedding event was caused by the inability of the rovers to perceive the terrain beneath the thin surface duricrust layer. Since the rovers relied on visual assessment and characterisation of the terrain, which appeared similar to surrounding areas, they were unaware of the hazards. Although the

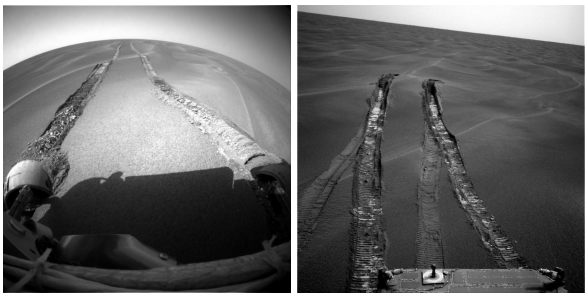
Figure 2. MER Opportunity stuck at Purgatory Dune in 2005 (left – Front Hazcam, Sol 449) and retreating after becoming free (right – Navigation Camera, Sol 491). Note the colour of the regolith in the wheel tracks, indicative of different soil beneath the thin duricrust [5].

duricrusts could not support the mass of the rovers, the thin, brittle layers were sufficient to support, and be formed by, wind-blown surface dust and small soil particles (aeolian sediment transport), which contributed to the camouflaging effort. When such duricrusts conceal loose soil underneath, a hazard exists; although, it is also possible for the duricrusts to form on more solid layers, such as bedrock.

Such visual means of estimating soil properties, although rapid, have shown themselves to be insufficient for accurately identifying safe and unsafe terrain in environments where concealing duricrusts are present. Instead, direct-sensing techniques, such as cone penetrometer, dynamic plate, and bevameter testing provide more accurate and useful indications of sub-surface terrain conditions [7]. Each of these example methods penetrates or impacts the terrain to determine sub-surface properties, such as load bearing capabilities, which allows for a reliable assessment of the ability for the soil to support a rover.

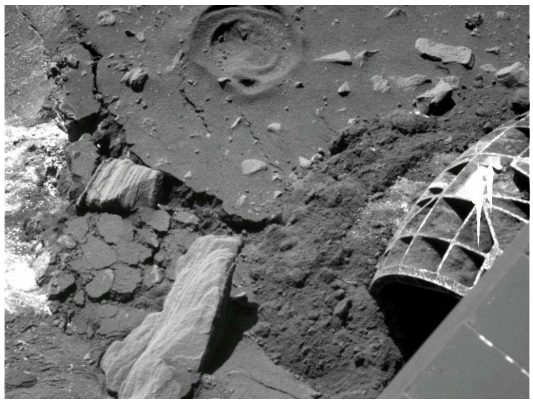
Figure 3: Martian terrain as viewed by the MER Spirit Pancam (Sol 2190). Note the cracked and crumbled surface duricrust and the loose soil beneath [13].

As mentioned above, duricrusts are relatively thin layers of indurated soil that seem to ubiquitously cover the surface of Mars, according to several published observations of the planet [3][8][9][10]. There is still some speculation as to the exact formation process of these crusts on the Martian surface, although it is held that the most-likely cause is due to microscopic layers of moisture on the surface of aeolian particles. This moisture comprises dissolved salts and other compounds that create weak bonds through precipitation of minerals through evaporation or other processes with neighbouring particles. As more material is deposited on existing cemented material, the layer becomes thicker. Since this process involves wind-deposited material, the crusts are extremely weak and prone to fracture and crumbling by the same wind. As such, many of the identified duricrusts on the Martian surface are relatively thin [3][12][13] (Fig. 3).

Another formation method for duricrusts would be for ground moisture, which contains similar dissolved salts and other compounds, to evaporate and leave behind a weakly cemented soil surface. Although this is a common occurrence on Earth, where ground moisture is abundant, the low moisture content of Mars may make this formation method slightly less likely. These two methodologies are both speculative, however, and neither method has been conclusively shown nor disproved [14].

Some support for the relative weakness for these duricrusts can be seen by the low moisture content on Mars. As indicated by several sources, the soil and atmospheric water content is only between 2 – 11%. According to the data generated by the Viking lander missions, a very low water content was discovered, approximately 2 – 4%, although the Viking instruments were not specifically calibrated for such tests [15]. Later reports show evidence of higher water content on the planet, citing 10% relative humidity from Viking mission orbiter data [16] and 9 – 11% as predicted by the hydrogen content observed by the Odyssey orbiter [3]. These small quantities of moisture can only appear to be capable of supporting small amounts of dissolved salts, which in turn form very weak duricrusts. Our laboratory experiments, described in the following sections, support this observation by showing a clear relationship between duricrust strength and initial moisture content.

2. DURICRUST CREATION

Many of the past remote missions to Mars have identified the chemical composition of the Martian soil at several locations on the planet. Yen et al [17] compiled much of these data beginning with the early Viking missions of the 1970s and Ruff et al [18] focused on the NASA MER Spirit and Opportunity missions around Gusev crater and Meridiani Planum. These data reflected the observed compositions of rocks and soils on the surface, identifying nearly a dozen notable chemical compounds and mineralogical components.

Due to the extensive nature of these analyses, a subset of chemical compounds was chosen to create simulated duricrust compositions in a laboratory environment. Similarly, the analysis of the 'bright dust' portion of the terrain was selected to represent the artificial duricrusts. These selections led to the following elements and proportions used for the experiments presented in this paper (Tab. 1). The lesser abundant compounds identified in the Martian surface were omitted from these trials and the main compound amounts were normalised based on their weighted presence in the soil.

Table 1: Artificial duricrust compounds and mass proportions used for laboratory experimentation

Si (%)	Fe (%)	$MgSO_4$ (%)	Al (%)
52.2	19.8	17.3	10.8

It should be noted that although there is a column labelled 'Fe', two types of iron oxide were used during the experiments: magnetite (Fe_3O_4) and haematite (Fe_2O_3). Each oxide was used during different experiments since each of these compounds have been found in Martian soil. For some of the experiments an even mixture of both oxides was also used. The oxides used for each test will be clearly identified in the presented data.

The iron oxides, both magnetite and haematite, and the aluminium components were sourced as fine, pure powders. The magnesium sulphate was purchased as food-grade Epsom salts and appeared as small crystals (<3mm), which were pulverised prior to use. These elements were measured by mass based on their identified proportions (Tab. 1) and combined thoroughly using a hand rake to form a dry mixture. The resulting dry mixture was then incorporated with the silicon as SiO_2 in the form of sand.

the duricrust mixture. The amount of water applied and the duricrust thickness were recorded for each sample preparation.

Samples were typically prepared as two sets of three, for 4-7 days in order to ensure that the applied, and general atmospheric, water had evaporated, allowing at least four days were required for the entirety of the duricrust used due to time availabilities, but it was noted that to cure. Longer durations were sometimes duricrust to form a weakly cemented layer atop the loose SSC-3 simulant. It was found experimentally, that where each set had similar water content and duricrust thickness. After preparation, the samples were placed under a plastic shroud in an area with a dehumidifier at room temperature (Fig. 6, right). The samples were left

The silicon component comprised a relatively fine (~100-212µm), sub-angular sand acquired from wind-swept dunes at West Wittering Beach in the south of England. This soil simulant was dubbed SSC-3 (Fig. 5). The sand was chosen for its grain size and shape, being similar to some soil particulates observed on the Martian surface around Gusev crater [19], and also for its availability in bulk. Laboratory analysis of SSC-3 was conducted and found the soil simulant to have a rather narrow selection of grain size, which eliminated the need for extensive processing prior to its use in the duricrust experiments. This uniform grading of the simulant is a characteristic of aeolian sands, such as those found in the Martian surface regolith.

Once the dry mixing process was complete, in a single batch for a series of six samples (for homogeneity of the mixture amongst the trial set), the mixture was applied to the surface of a set of 9L buckets (Fig. 6, left) partially filled with loose SSC-3 (approximately 1.45g/cc, roughly the loosest natural state for the simulant with a density range of about 1.42g/cc – 1.62 g/cc). The base-layer SSC-3 soil was poured into the buckets from a height of ≥0.5m, allowing the soil particles to achieve terminal velocity and resulting in the desired low density [20]. The density of the base-level soil was calculated by volume.

The dry duricrust mixture was applied to the surface of the SSC-3 simulant in 4-6 layers by gently sprinkling the mixture onto the prepared loose simulant in order to achieve a relatively uniform-thickness layer. After each layer was applied, the duricrust mixture was hydrated using distilled water in a fine-sprayed mist. The amount of water dispensed per layer was calculated to have a desired final percentage of water, by mass, relative to longer curing times didn't affect the behaviour and performance of the duricrusts; that is, once the duricrust was cured, additional resting time did not alter its physical characteristics.

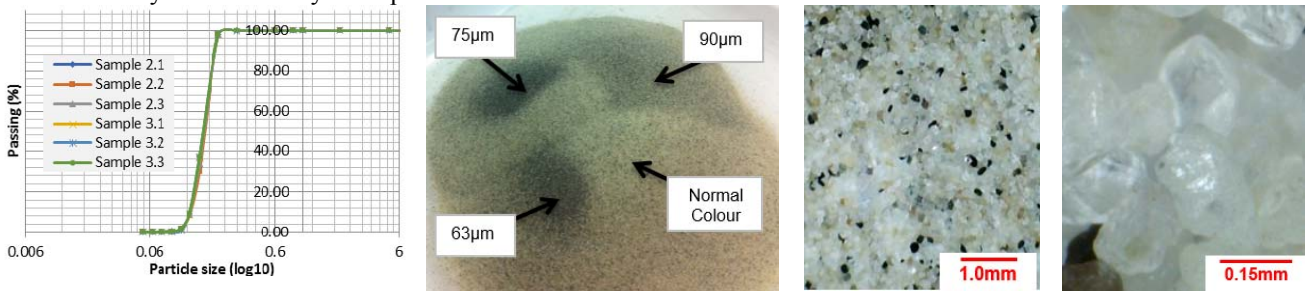

a) b) c) d)

Figure 5: SSC-3 soil simulant analysis and images. a) Sieve analysis results showing that about 98% passes the 212µm sieve; 35% passes the 150µm sieve; 12% passes the 125µm sieve; and <4% passes the 106µm sieve. These results show that nearly all of the naturally-occurring SSC-3 simulant has particle sizes in the range of 100-212µm. b) 1x image, c) 33x image, d) 400x image of SSC-3.

Figure 6: Freshly-prepared bucket sample using red Fe_2O_3 iron oxide (left). Several prepared samples using black Fe_3O_4 iron oxide curing under the plastic shroud with a dehumidifier (right).

Due to financial constraints, multiple components, and time required to prepare duricrust analogues using the elements identified in the Martian soil, alternative duricrust creation methods were investigated. Beyond the iron oxide experiments, an additional dozen tests were performed using Ordinary Portland Cement (OPC) as the simulant binding agent. These tests were done in order to find a similar physical analogue to the Martian duricrusts that were created in the main portion of this research. Two different proportions of cement were added to SSC-3 as a dry mixture with soil:cement ratios of 50:1 and 25:1. As before with the iron oxideexperiments, the dry mixture was applied to the surface of low-density SSC-3 in multiple layers, with each layer prompting water application with a spray bottle filled with distilled water. Variations in the number of layers (4, 6, or 8), duricrust thickness (9 – 24mm), and water content (ranging from 5.66 – 32.75%) comprised the experimental features that were altered.

3. EXPERIMENTAL SETUP

Duricrust samples were prepared in 9L buckets using loose SSC-3 soil simulant as the substructure and duricrusts formed on top of this layer, as described in Section III. A variety of combinations of iron oxide type, duricrust thickness, and % water content were used (Fig. 7). Due to the early, informal trials that showed Fe_3O_4 to produce stronger duricrusts than Fe_2O_3, more emphasis was placed on this iron oxide. It was hoped that a notable load-bearing duricrust could be created as a result of these experiments, in addition to quantifying some of the duricrust physical properties.
Strength of the formulated duricrusts was determined as the apparent soil density, as compared to natural SSC-3, and it was measured by use of a dropped-mass Dynamic Cone Penetrometer (DCP) (Fig. 8). This device was empirically calibrated to the range of natural densities found using the SSC-3 soil simulant (approximately 1.42g/cc – 1.62 g/cc). Penetration-per-Impact and volumetric soil density data were recorded and a curve was fitted for use as the equation to derive density from the depth of each impact (Fig. 9). Note that each of the data points shown in Fig. 9 are averaged values of five experiments performed at each general density: low (about 1.47g/cc); medium (about 1.52g/cc); and high

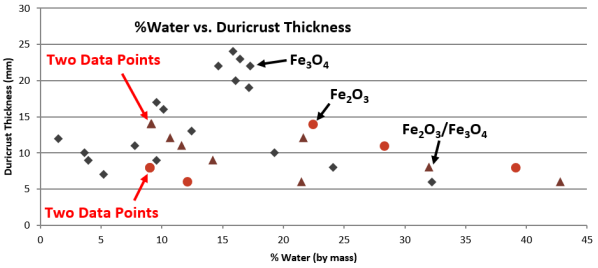

Figure 7: Duricrust experiment criteria for the 33 trials, sorted by iron oxide formulation: pure Fe_3O_4, a mixture of 50% Fe_2O_3 and 50% Fe_3O_4, and pure Fe_2O_3.

(about 1.69g/cc). The cone design of the DCP was based closely on one of the ASTM standard cone penetrometers, which has a cone diameter of 35.7mm and an interior cone angle of 60°. Given the similarity in design, it was planned that other existing, terrestrial, analysis methods could be employed, if needed. DCP specifications are listed below in Tab. 2.

Impact Num	Depth	Density
0	≤ 37.875mm	0.0140*depth + 2.0490
	> 37.875mm	0.0014*depth + 1.5716
1	≤ 31.000mm	0.0113*depth + 1.8693
	> 31.000mm	0.0026*depth + 1.5986
2	≤ 15.250mm	0.0194*depth + 1.8142
	> 15.250mm	0.0055*depth + 1.6021
3	≤ 13.000mm	0.0309*depth + 2.0490
	> 13.000mm	0.0070*depth + 1.6090
4	≤ 10.000mm	0.0324*depth + 1.8417
	> 10.000mm	0.0059*depth + 1.5767
5	≤ 8.250mm	0.0523*depth + 1.9495
	> 8.250mm	0.0042*depth + 1.5529

DCP Penetration-per-Impact values and SSC-3 volumetric soil density values were averaged over a set of twelve calibration samples of varying SSC-3 densities: 3 low; 3 medium; and 3 high, in order to create the six soil density-from-depth algorithms. Due to their unique behaviours, a separate algorithm was used for each of the first five impacts and an additional algorithm for the self-weight (zeroth) sinkage (Tab. 3). Each measurement cycle began with the self-weight assessment where the DCP was gently placed onto the
Table 3: DCP algorithms for converting Penetration-per-Impact sinkage to SSC-3 soil densitysoil surface and allowed to sink under its own weight, with no impact or external downward force applied. The dropped-mass impact hammer was then raised to the height of the shaft collar and then released with the guide rod of the DCP allowing it to freely move vertically. This impact process was repeated for approximately 20 impacts, or until the bottom of the sample bucket was reached. Although the DCP was driven to the bottom of the sample buckets, only the first five impacts were used to gauge the density of the duricrust or underlying soil, as it was shown during

Table 2: DCP device specifications

Total mass	Dropped mass (m)	Drop height (h)	Stopping Distance (s)	Impact Force (F)	Cone Diameter
1.37 kg	0.553 kg	0.22 m	0.00265 m	237.43 N	30 mm

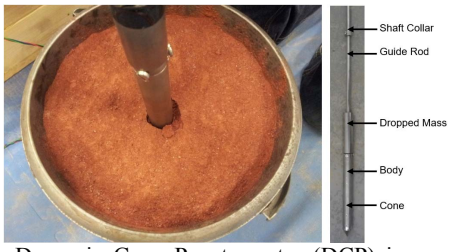

Figure 8: Dynamic Cone Penetrometer (DCP) in use testing a duricrust sample (l). Photo of the DCP with labelled parts (r).

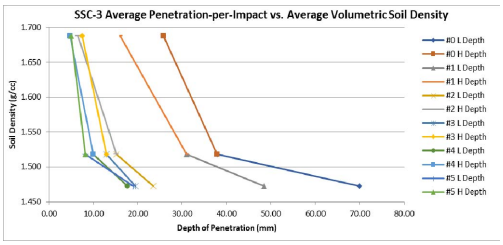

Figure 9: Depth of Penetration vs. Soil Density for the SSC-3 soil simulant as measured by DCP.

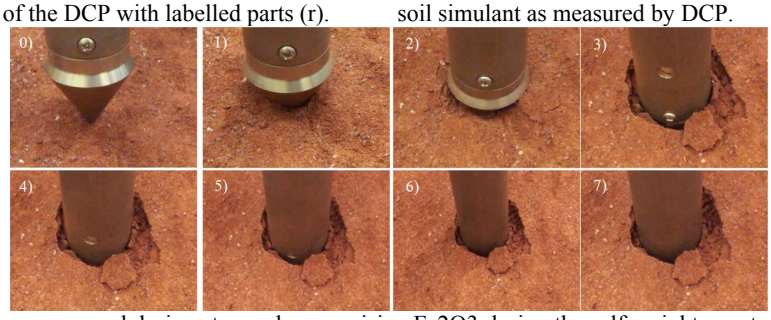

Figure 10: DCP impacts on a prepared duricrust sample comprising Fe2O3 during the self-weight penetration, 0, and the first seven impacts, 1 – 7. The duricrust had a thickness of 11mm and was created with a water content of 22.23%. This sample presented a relatively strong duricrust as noted by the DCP requiring four impacts to completely penetrate the crust. The self-weight penetration was very small at only 2mm. Impacts #1 and #2 show the DCP still within the crust. Impact #3 shows the DCP tip exiting the duricrust whilst the DCP body remained within the crust thickness. Impacts #4 – #7 show the DCP body beyond the crust.

Figure 11: Post-experiment duricrust analysis of two Fe_2O_3 samples. (left) 8mm crust thickness with 9.06% water added by mass. (right) 8mm crust thickness with 39.24% water added by mass. The lower water content sample, left, produced a weak, crumbly crust and the higher water content sample, right, produced a strong, solid crust.

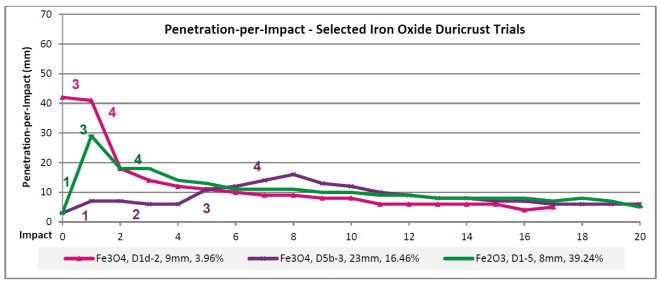

Figure 13: DCP Penetration-per-Impact subsets. The increase in values from impact #5 through #8 for D5b-3 is initiated by the DCP fully penetrating the lower limit of the duricrust. D1d-2 showed the duricrust failing from the onset, such that there is monotonically decreasing values through the trial. D1-5 presented a strong but brittle duricrust, as evidenced by the low self-weight penetration and much higher subsequent values. The numbered sections correspond to DCP penetration stages, as in Fig. 14. D1d-2 did not experience Stages 1-2, beginning directly with Stage 3; and D1-5 did not exhibit Stage 2.

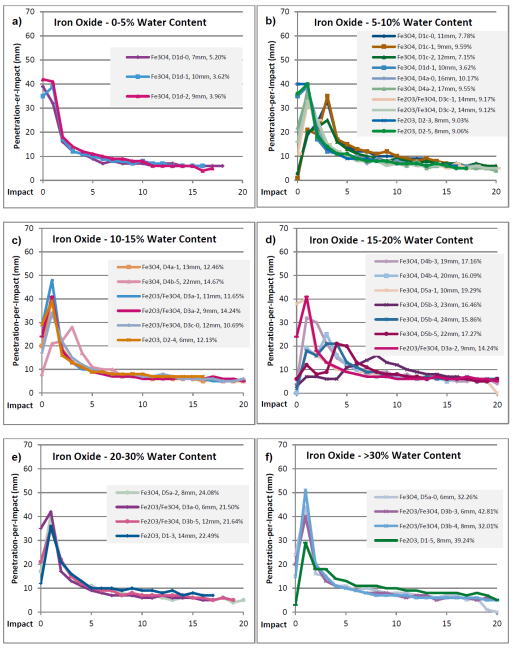

Figure 12: DCP Penetration-per-Impact graphs showing all 33 of the iron oxide duricrust experiments, indicating duricrust thickness and water content, and sorted by water content. Note that around Impact #5, each of the trials behaves similarly for the remaining impacts. This similarity of Penetration-per-Impact is due to the relatively-common soil pressure acting above the DCP cone, and the duricrust is no longer a factor in the DCP penetration.

experimentation that repeated impacts produced indistinguishable differences between varying soil densities after this point (Fig. 12). During each experiment, the cycle of impact was recorded to video and photographs were captured after each impact. The self-weight and first seven impacts of a Fe_2O_3 sample are shown in Fig. 10.

After each experiment was performed, the duricrusts were sectioned for analysis and portions were kept in storage for later illustrative purposes (Fig. 11).

4. RESULTS

Data from the duricrust experiments was captured and combined into two main formats for analysis: Penetration-per-Impact (Fig. 12), where there self-weight and individual sinkage values for each impact were plotted; and Total Depth of Penetration (Fig. 15), where the accumulative total sinkage of the DCP was shown versus the number of impacts.

The DCP Penetration-per-Impact graph (Fig. 12) shows extremely unique information amongst the samples for the self-weight sinkage and the first 4 – 5 impacts. The Penetration-per-Impact beyond this point generally becomes quite similar for each of the samples, regardless of duricrust preparation. This is due to DCP cone proceeding beneath the duricrust for most of the samples, where the underlying soil preparation is nearly identical. However, for SSC-3 preparations where the soil density varied, as was the case during the DCP calibration experiments, the Penetration-per-Impact still remained similar throughout the test beyond the fifth impact. This is due to the loading effects of the soil above the DCP cone having a greater effect on penetration than the density of the soil local to the cone itself. Because of this, all density calculations only considered the self-weight and first five impacts.

What is most noteworthy in Fig. 12 is the great disparity in the self-weight sinkage values, ranging from 0mm – 42mm. Equally broad in values are the depths for the first impact. In each of these cases, the duricrust strength had a leading influence. Although higher water content led to stronger duricrusts, the thickness of the crust also played a key role. Strong, thick duricrusts withstood repeated impacts before allowing the DCP cone to entire pass beyond, as is shown for sample Fe_3O_4, D5b-3, 23mm, 16.46% (Fig. 13, purple line with x-shaped markers). This sample began with a low self-weight penetration of only 3mm and the first four impacts were: 7mm, 7mm, 6mm, and 6mm, respectively. It was only until Impact #5, with a Penetration-per-Impact of 11mm that the entire DCP cone was nearly beyond the duricrust.

In comparison, other samples with noticeably weak duricrusts showed signs of failure beginning with the self-weight sinkage. An extreme example was sample Fe_3O_4, D1d-2, 9mm, 3.96% (Fig. 13, fuchsia line with triangle markers). This experiment began with the highest self-weight sinkage of 42mm and continued with high sinkage values for the following impacts. The depths of these initial impacts are about 1/2 – 2/3 of those found for SSC-3 of similar density as the underlying soil, but without the duricrust. This shows that although the duricrust was easily penetrated, it did have an effect on the penetration of the DCP. In some experiments, the duricrust fractured quickly and shards of crust preceded the DCP cone during penetration, resulting in somewhat misleadingly lower Penetration-per-Impact values.

Fig. 15 shows the Total Depth of Penetration results for the duricrust experiments. Although this graph is quite dense, it presents two notable trends in the behaviour of the samples: those samples whose duricrust presented a difficultly or reduced ease of penetration (Fig. 15, label 1); and those whose duricrust presented little or no resistance (Fig. 15, label 2).

The compound curves of Fig. 15 (label 1) show the self-weight sinkage leaving only the DCP cone tip slightly penetrating the duricrust (Fig. 14, 1) and requiring several impacts for the full cone to enter the crust layer (Fig. 14, 2 and 3) before finally penetrating the duricrust completely (Fig. 14, 4). This is illustrated by a low initial penetration and gradually-increasing Penetration-per-Impact values. The change in the plot curves from a downward arc to an upward one represents the point where the entire cone had travelled beyond the duricrust and only encountered the loose SSC-3 simulant beneath.

Weak duricrusts behaved in one of two ways. Either the crust was generally very weakly cemented, in which case the DCP quickly progressed to Fig. 14, 3 or Fig. 14, 4, as the duricrust could not withstand the self-weight and early impacts of the DCP. The other case was where the duricrust may have been more strongly cemented, however it was too thin and brittle to support the DCP and rapidly shattered. For the first scenario, the DCP easily penetrated the sample and the data curves appeared similar to those experienced when no duricrust was present (e.g. Fe_3O_4, D1d-2, 9mm, 3.96%, Fig. 13). The second case, where the crust was simply too thin, can be seen in examples such as Fe_2O_3, D1-5, 8mm, 39.24% (most clearly shown in Fig. 13, green line with horizontal bar markers). Despite the high water content of this sample, which generally resulted in stronger duricrusts, the thinness of the layer was insufficient to resist the DCP.

Following the iron oxide experiments, a dozen tests were performed using Ordinary Portland Cement as the duricrust binding agent in order to find a suitable physical analogue with similar strength and density characteristics as those found with the recreated Martian duricrusts.

For field testing and large-scale laboratory testing purposes, the artificial duricrusts created with Ordinary Portland Cement proved to be a suitable physical substitute for the crusts fabricated with Martian-

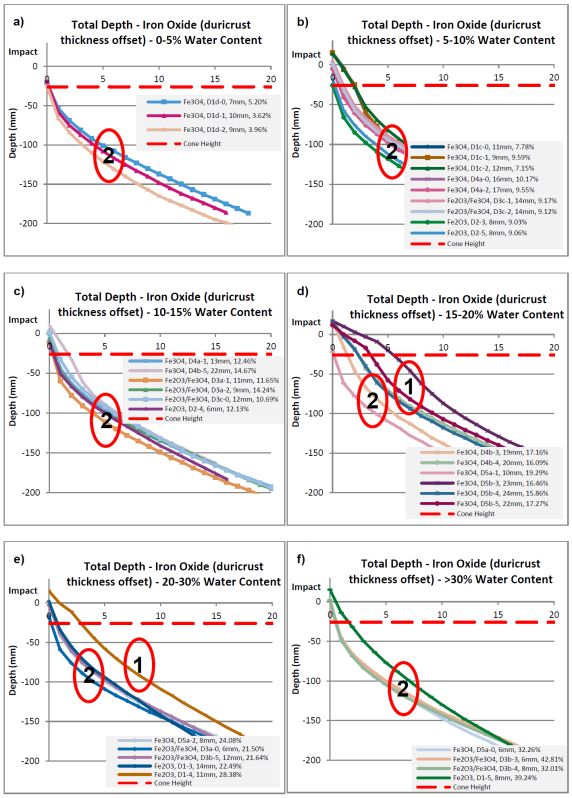

Figure 15: DCP Total Depth of Penetration graph showing all 33 of the iron oxide duricrust experiments, indicating duricrust thickness and water content. The compound curves (1 - downward then upward) of the upper lines indicate the noted effect of the duricrust for those tests. Simple curves (2 - upward curve only) of the lower lines indicate that the duricrust was not well observed or that it failed early in the testing, either due to a low water content or a small crust thickness.

identified components. The low-cost nature of the cement (see Tab. 4) and the close performance to the Martian duricrusts make it a good alternative when only physical characteristics are being tested.

Weak and easily penetrated duricrusts were observed for samples with low water content, independent of crust thickness. These samples possessed crumbly surfaces that failed instantly, or near-instantly during testing. It should be noted that these low-water content samples (<10% water) represent similar amounts of water observed by previous and current Mars missions [3][15][16].

Given the performance of the laboratory-created duricrusts, many of their behaviours were qualitatively similar to terrain already encountered on Mars by current and past rover missions, notably the low-water content samples and the thin crust samples. The higher strength of the duricrust samples with higher water content and thicker crusts are less-likely to be observed on Mars, but even they did not last under repeated DCP loads and need to be treated with caution if encountered. Based on these test results and the presented data, it

Table 4: Duricrust costs (excluding silicon component)

Component	Per 100g Comp.	Per 100cc Duricrust
Fe_2O_3	£2.00	£0.40
Fe_2O_3	£2.40	£0.48
Fe_2O_3	£1.20	£0.13
$MgSO_4$	£0.15	£0.03
Total Cost (Martian Duricrust)		**£0.60**
OP Cement	£0.09	£0.0037
Total Cost (Artificial Duricrust)		**£0.0037**

would be prudent to employ direct-measurement methods to ensure sufficient traversability of the terrain, such as those systems investigated during the FASTER project [7], which would allow future Mars rover missions to traverse the surface with a much higher degree of confidence and certainty than in the past.

5. CONCLUSION

This paper has presented a means for artificially creating Mars-like duricrusts in a terrestrial laboratory environment. Realistic duricrust compounds based on those identified on the Martian surface were used during their creation, such as silicon, magnesium sulphate, iron oxide, and aluminium. Thirty-three samples were created using a variety of iron oxide type (magnetite – Fe_3O_4 and haematite – Fe_2O_3), duricrust thickness (ranging from 6 – 24mm), and water content (ranging from 3.62 – 42.81% by mass).

The resulting crusts were tested using a Dynamic Cone Penetrometer (DCP), calibrated to the silicon component, a soil simulant called SSC-3, which is comprised mainly of 150 - 212µm sub-angular particles of quartz (SiO_2). The laboratory-created duricrusts presented several types of behaviour, such as weak and crumbly – easily penetrated, thin and brittle – easily penetrated, and relatively strong but still susceptible to penetration. Using the DCP, the duricrust samples were classified by their density, or resistance to penetration, in numbers relative to those found in natural SSC-3 (i.e. the normal range of simulant densities, 1.42 – 1.62g/cc, without a surface duricrust).

Weak crusts and brittle crusts displayed higher relative densities that the loose soil preparations on which they rested, showing that even easily penetrated duricrusts can still be distinguished from pure, loose soil. Stronger crust samples showed their presence more so by resisting initial penetrations by the DCP. The strongest of the duricrust samples demonstrated themselves by resisting several DCP impacts before the testing device moved below the crust layer. With this last set of samples, cone penetration results very clearly showed the presence of a surface duricrust.

In all of these tests, the duricrust samples were penetrated within five impacts of the DCP, indicating that although they may be relatively weak or strong, as compared to a natural soil simulant, they all represented potential hazards to traversing a terrain covered by such layers. As a result, a key finding to this study is the

recommendation of direct-sensing instrumentation on future Mars rovers, to ensure suitable trafficability of the surface.

During the course of these tests, an economical physical analogue to the duricrusts fabricated using the Martian-identified components was also tested. By using Ordinary Portland Cement in very low proportions to a soil simulant (25:1), a physically-similar duricrust can be created. This provides an optional duricrust creation method for large-scale testing, such as rover prototypes trials during field tests or within spacious laboratory facilities. At 1/160th of the cost, OPC is a viable economic and physical alternative with very similar performance characteristics to duricrusts created using the Martian-identified elements.

REFERENCES

1. V. G. Perminov, (July 1999). “The Difficult Road to Mars - A Brief History of Mars Exploration in the Soviet Union.” NASA Headquarters History Division. pp. 34–60.
2. Wikipedia. (2014) “Mars 3,” World Wide Web, http://en.wikipedia.org/wiki/Mars_3, October 19, 2014.
3. D. T. Vaniman, D. L. Bish, S. J. Chipera, C. I. Fialips, J. W. Carey, and W. C. Feldman (2004). “Magnesium Sulphate Salts and the History of Water on Mars,” Nature, Vol. 431, pp. 663–665, 7 October 2004.
4. H. J. Moore and B. M. Jakosky (1989). “Viking landing Sites, Remote-Sensing Observations, and Physical Properties of Martian Surface Materials,” Icarus, 81, 164–184.
5. Mars Exploration Rover Mission, World Wide Web, http://marsrovers.nasa.gov/home/, accessed 2007.
6. Mars Exploration Rover Mission: All Spirit Updates, “Spirit Updates: 2009”, World Wide Web, http://mars.nasa.gov/mer/mission/status_spiritAll_2009.html, accessed October 2014.
7. W. A. Lewinger, F. Comin, S. Ransom, L. Richter, S. Al-Milli, C. Spiteri, Y. Gao, M. Matthews, and C. Saaj (2013). “Multi-Level Soil Sensing Systems to Identify Safe Trafficability Areas for Extra-Planetary Rovers,” 12th Symposium on Advanced Space Technologies in Robotics and Automation (ASTRA 2013), ESA/ESTEC: Noordwijk, The Netherlands, May 15-17, 2013.
8. B. M. Jakosky and P. R. Christensen (1986). “Global Duricrust on Mars: Analysis of Remote-Sensing Data,” J. Geophys. Res., 91(B3), 3547–3559.
9. C. D. Cooper and J. F. Mustard (2002). "Spectroscopy of Loose and Cemented Sulfate-Bearing Soils: Implications for Duricrust on Mars,” in Icarus, Volume 158, Issue 1, July 2002, Pages 42–55.
10. Scientific American Editors (2012). Exploring Mars: Secrets of the Red Planet, Macmillan. Aug. 31, 2012.
11. N. Barlow (2008). Mars: An Introduction to its Interior, Surface and Atmosphere. Cambridge University Press, 10 Jan 2008.
12. Alien Textures ‘Weird Stuff’ – Geologists Just Scratching the Surface, Astrobiology Magazine, World Wide Web, http://www.astrobio.net/topic/solar-system/mars/alien-textures-weird-stuff/, January 7, 2004.
13. Mars Exploration Rover Mission: Multimedia: All Raw Images: Spirit: Panoramic Camera: Sol 2190, World Wide Web, http://mars.nasa.gov/mer/gallery/all/2/p/2190/2P320875822EFFB27MP2400L7M1.HTML, accessed 2010.
14. J. F. Mustard and C. D. Cooper (1999). "Layering Due to Pedogenic Processes in Martian Soil, in 5th International Conference on Mars, Abstract 6168. Lunar and Planetary Institute, Houston (TX), USA, 1999.
15. A. S. Yen, B. C. Murray, and G. R. Rossman (1998).”Water Content of the Martian Soil: Laboratory Simulations of Reflective Spectra,” in J. Geophysical Research, Vol. 103, No. E5, pp 11,125–11,133, May 25, 1998.
16. H. Savijarvi (1995). “Mars Boundary Layer Modeling: Diurnal Moisture Cycle and Soil Properties at the Viking Lander 1 Site,” in Icarus 117, 120-127 (1995).
17. A. S. Yen, R. Gellert, C. Schröder, R. V. Morris, J. F. Bell III, A. T. Knudson, B. C. Clark, D. W. Ming, J. A. Crisp, R. E. Arvidson, D. Blaney, J. Brückner, P. R. Christensen, D. J. DesMarais, P. A. de Souza Jr., T. E. Economou, A. Ghosh, B. C. Hahn, K. E. Herkenhoff, L. A. Haskin, J. A. Hurowitz, B. L. Joliff, J. R. Johnson, G. Klingelhöfer, M. B. Madsen, S. M. McLennan, H. Y. McSween, L. Richter, R. Rieder, D. Rodionov, L. Soderblom, S. W. Squyres, N. J. Tosca, A. Wang, M. Wyatt, and J. Zipfel (2005). “An Integrated View of the Chemistry and Mineralogy of Martian Soils,” in Nature, Vol. 436, 7 July 2005.
18. S. W. Ruff, P. R. Christensen, T. D. Glotch, D. L. Blaney, J. E. Moersch, and M. B. Wyatt (2008). “The Mineralogy of Gusev Crater and Meridiani Planum Derived from the Miniature Thermal Emission Spectrometers on the Spirit and Opportunity Rovers”, The Martian Surface: Composition, Mineralogy, and Physical Properties. Ed. J. F. Bell III, Cambridge University Press, 2008.
19. N. A. Cabrol, K. E. Herkenhoff, R. Greeley, E. A. Grin, C. Schröder, C. d’Uston, C. Weitz, R. A. Yingst, B. A. Cohen, J. Moore, A. Knudson, B. Franklin, R. C. Anderson, and R. Li (2008). “Soil Sedimentology at Gusev Crater from Columbia Memorial Station to Winter Haven”, in Journal of Geophysical Research, Vol. 113, E06S05, 2008.
20. T. P. Gouache, C. Brunskill, G. P. Scott, Y. Gao, P. Coste, and Y. Gourinat (2010). “Regolith Simulant Preparation Methods for Hardware Testing”, in Planetary and Space Science, Vol. 58, Iss. 14, pp. 1977–1984, 2010.